Available online at www.sciencedirect.com
ScienceDirect
Virology 358 (2007) 321–333
VIROLOGY
www.elsevier.com/locate/yviro

Assembly of trans-encapsidated recombinant viral vectors engineered from Tobacco mosaic virus and Semliki Forest virus and their evaluation as immunogens

Mark L. Smith, Tina Corbo [1], Jacqueline Bernales [2], John A. Lindbo [3], Gregory P. Pogue [4], Kenneth E. Palmer, Alison A. McCormick *

Large Scale Biology Corporation, 3333 Vaca Valley Parkway, Suite 1000, Vacaville, CA 95688, USA

Received 1 June 2006; returned to author for revision 6 July 2006; accepted 23 August 2006
Available online 2 October 2006

Abstract

RNA virus vectors are attractive vaccine delivery agents capable of directing high-level gene expression without integration into host cell DNA. However, delivery of non-encapsidated RNA viral vectors into animal cells is relatively inefficient. By introducing the tobacco mosaic virus (TMV) origin of assembly into the RNA genome of Semliki Forest virus (SFV), we generated an SFV expression vector that could be efficiently packaged (trans-encapsidated) *in vitro* by purified TMV coat protein (CP). Using cellular assays, pseudovirus disassembly, RNA replication and reporter gene expression were demonstrated. We also evaluated the immune response to trans-encapsidated recombinant SFV carrying a model antigen gene (β-galactosidase) in C57/B6 mice. Relative to RNA alone, vector encapsidation significantly improved the humoral and cellular immune responses. Furthermore, reassembly with recombinant TMV CPs permitted the display of peptide epitopes on the capsid surface as either genetic fusions or through chemical conjugation, to complement the immunoreactivity of the encapsidated RNA genetic payload. The SFV vector/TMV CP system described provides an alternative nucleic acid delivery mechanism that is safe, easy to manufacture *in vitro* and that also facilitates the generation of unique nucleic acid/protein antigen compositions.

Keywords: Tobacco mosaic virus; Reassembly; Semliki Forest virus; Pseudovirus; Antibody response; Cellular immune response; Alphavirus

Introduction

Genetic immunization against pathogen or tumor antigens has proven successful using DNA and modified virus vectors. As a result of intracellular protein expression and class I antigen presentation, such vaccines often demonstrate superior abilities to stimulate high levels of cellular immune responses, when compared with protein antigens of extracellular origin. The simplest approach to gene therapy is the injection of naked plasmid DNA, yet due to the inefficiency of cellular uptake (Nishikawa and Huang, 2001), a high dose of plasmid is required to stimulate immunity, which has posed a challenge for widespread use (Hoare et al., 2005; Levy et al., 2000). Concerns have also been raised regarding the possibility of genomic integration and resulting cellular transformation events. Extensive animal testing has indicated that the likelihood of plasmid incorporation into host DNA is low (Martin et al., 1999; Vilalta et al., 2005). However, a recent study (Wang et al., 2004) evaluating strategies for improved plasmid delivery resulted in multiple independent genomic integration events, suggesting that a balance between efficacy and safety must be considered.

One alternative to DNA vaccination are RNA virus vectors (Lundstrom, 2002) such as Semliki Forest virus (SFV) based

* Corresponding author. Fax: +1 707 446 3917.
E-mail address: alison.mccormick@myifp.com (A.A. McCormick).
[1] Present address: Genentech, 1 DNA Way, South San Francisco, CA 94080, USA.
[2] Present address: Alta Analytical Laboratory, Inc., 1100 Windfield Way, El Dorado Hills, CA 95762, USA.
[3] Present address: Department of Plant Pathology, The Ohio State University, Ohio Agricultural Research and Development Center, 24 Selby Hall, 1680 Madison Ave., Wooster, OH 44691, USA.
[4] Present address: Office of Technology Commercialization, University of Texas at Austin, 3925 W. Braker Lane, Suite 1.9A, Austin, TX 78759, USA.

0042-6822/$ - see front matter © 2006 Elsevier Inc. All rights reserved.
doi:10.1016/j.virol.2006.08.040

vectors (Zhou et al., 1994). Relative to DNA vectors, RNA virus vectors show transient persistence (Morris-Downes et al., 2001), have a comparable or superior ability to deliver pathogen and tumor antigen genes in animal models to either prevent or cure disease (Lundstrom, 2002; Lundstrom, 2005) and do not integrate into chromosomal DNA. For immunizations, the SFV RNA can be either used directly or packaged into recombinant replication-deficient SFV particles (Berglund et al., 1993). The current process of manufacturing SFV particles via transient transfection procedures is both difficult to scale and may result in replication competent virus, although improvements to the system have reduced the likelihood of recombination (Smerdou and Liljestrom, 1999). One recently reported alternative is to encapsidate SFV-based RNA vectors using the vesicular stomatitis virus glycoprotein (VSV-G) in place of the SFV structural proteins, as there is no sequence homology between VSV-G and the SFV vector genome. However, the culture conditions for this system remain problematic (Dorange et al., 2004). We therefore investigated alternative packaging strategies for the SFV replicon, by employing the capsid of a distantly related member of the alphavirus superfamily, Tobacco mosaic virus (TMV).

To evaluate this approach, we incorporated the TMV origin of assembly (Oa) into a SFV replicon containing the beta-galactosidase (β-gal) reporter gene. Packaging of the RNA then occurs simply by mixing purified coat protein (CP) with modified SFV RNA *in vitro*. RNA-directed self-assembly results in the efficient *in vitro* manufacturing of trans-encapsidated SFV pseudovirus in amounts directly proportional to RNA concentration when CP is in excess. To further expand this delivery system, we considered encapsidation with recombinant CPs, to introduce functionality to the pseudovirion capsid. As examples, the SFV replicon was combined with a TMV CP displaying an integrin-binding motif and a CP displaying a surface-exposed lysine. The latter facilitates the conjugation and co-delivery of peptides or whole protein (Smith et al., 2006) with the genetic payload, to create "bi-functional" pseudovirion vaccine compositions. For one such bi-functional vaccine, we complemented the encapsidated RNA with a surface-displayed T-cell peptide epitope derived from β-gal. Interestingly, the immune response to the combination of nucleic acid and protein antigen was skewed completely to the Th1 cellular response. The methods described can be easily extended to RNA encoding any biological activity including cytokines, chemokines, multiple target RNAs, encapsidated by any number of CP modifications with the desired immunomodulatory function(s).

Results

Assembly and characterization of pseudovirions and virus-like particles

TMV capsid formation is initiated by the interaction of CP subassemblies with a ~300 nt stem–loop structure internal to the genomic RNA (the origin of assembly; Oa) that has been well defined (reviewed in Butler, 1999). The CP is incorporated predominantly as two-ring 'disks' during elongation towards the 5′ RNA terminus (illustrated schematically in Fig. 1A), while elongation towards the 3′ terminus employs smaller aggregates.

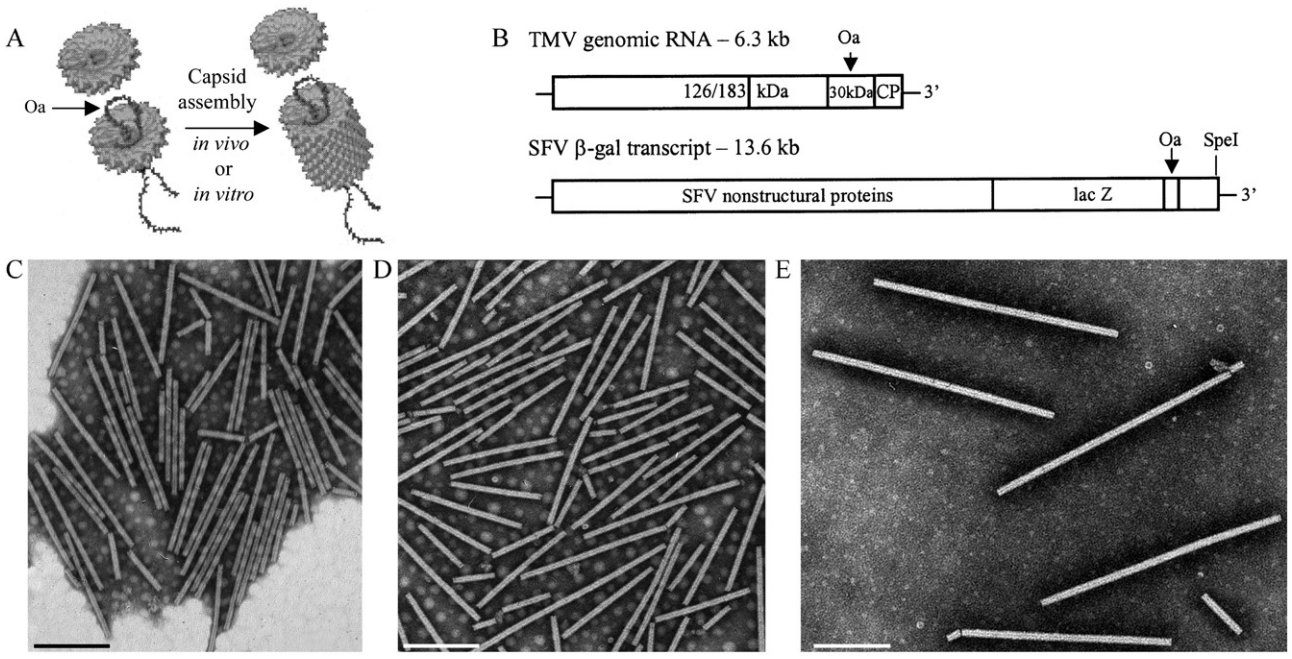

Fig. 1. RNA scaffolds compatible with TMV CP reassembly. (A) Simplified schematic representation of TMV CP reassembly onto RNA containing the origin of assembly (Oa; Reproduced courtesy of G. Stubbs). (B) Size and structure of the + sense RNA transcripts employed as scaffolds; TMV genomic RNA and SFV lacZ construct expressing β-galactosidase (SFV β-gal). (C to E) Representative electron micrographs of the reassembly product obtained when the transcripts in panel B were combined with various TMV CP preparations. (C) TMV genomic RNA with U1 CP. (D) TMV genomic RNA with RGD CP. (E) SFV β-gal transcript with the lysine modified CP (LSB 1295.10). Scale bars represent 200 nm.

Although the initial nucleation event requires the Oa, the process of elongation is independent of RNA sequence (Turner et al., 1988). This feature permits the engineering of RNA sequences that can be efficiently assembled *in vitro*. We introduced the TMV Oa into a SFV vector lacking the SFV structural proteins and expressing the beta-galactosidase (β-gal) reporter gene (SFV β-gal). Transcripts from this vector generated an RNA replicon of approximately 13.6 kb, over twice the length of the TMV genome (Fig. 1B). Because this RNA does not express SFV structural proteins, it is movement-deficient but can efficiently replicate in animal cells. We combined SFV β-gal transcript and control TMV genomic RNA with either wild-type U1 CP or CP preparations generated from recombinant TMV peptide fusions (Table 1). When wild-type U1 CP was combined with TMV genomic RNA, we observed rods that were visually indistinguishable from TMV by electron microscopy (Fig. 1C). Although a distribution of lengths was present in the observed population, rods of the expected length (300 nm) predominated. Replacing the U1 CP with RGD CP, displaying the RGD-integrin binding motif that mediates viral cell entry (Magnusson et al., 2001), yielded a comparable reconstituted virion population (Fig. 1D), indicating that epitope addition did not alter the CP's reassembly properties. In the case for the SFV β-gal transcript, the observed pseudovirions were approximately double the length of the TMV rods, as expected (Fig. 1E).

To further characterize the reassembly process, we monitored the change in absorbance at 310 nm (OD_{310}; proportional to average rod length (Butler and Klug, 1971)) following CP addition (Fig. 2A). For the combination of wild-type U1 CP with TMV genomic RNA, an initial rapid rise in absorbance occurred during the first 15 min, followed by a more gradual asymptotic increase towards the absorbance of the virus reference, with virions present at the same molar concentration as the RNA scaffold. After a 4-h incubation, the reassembly product, virus control and genomic RNA alone were inoculated onto the local lesion host *N. xanthi* (Fig. 2B). We have noted repeatedly that isolated TMV genomic RNA generates significantly (20–50 fold) lower numbers of lesions relative to intact virus, as previously observed (Fraenkel-Conrat and Singer, 1959). With encapsidation, the lesion numbers were similar to the intact virus, providing a functional though qualitative assessment of the reassembly products. Reassembly profiles and local lesion numbers obtained with the RGD CP were comparable to the wild-type U1 CP control (Figs. 2C and D) although the asymptotic rise in OD appeared more gradual, indicating that for this particular peptide fusion, the displayed epitope did not negatively impact the reassembly properties of the CP.

We also sought to encapsidate RNAs with multiple CP-fusion proteins in order to generate pseudovirions that displayed multiple peptides on their surface. We accomplished this by combining two different CPs in a staged format. Fig. 2E shows a representative OD_{310} profile for this staged reassembly with the RGD and U1 CPs. The RNA was initially combined with the RGD CP at a 1:10 RNA to CP mass ratio, approximately half the requirement for complete RNA encapsidation. After 30 min, the majority of the free CP was exhausted and the absorbance reached a plateau. Electron microscopy confirmed that the capsids formed were incomplete, with only an estimated 2% of the rods measuring 300 nm (data not shown). When the U1 CP was added, its incorporation into the partially assembled capsids resulted in a stepwise increase in absorbance that was not observed in the control reaction where buffer alone was employed. With TMV genomic RNA as the scaffold, the extent of encapsidation could be determined qualitatively by the recovery of viral infectivity. For the staged combinations, a clear increase in lesion numbers was observed relative to reactions where only the first CP was present (Fig. 2F) and from electron micrographs, 35% of rods observed were full length (data not shown).

For encapsidation reactions, we typically employed a 30% excess of CP, similar to the 20–22:1 CP to RNA mass ratios employed by others investigating wild-type virus reconstitution (Fraenkel-Conrat and Singer, 1959; Stussi et al., 1969). To determine if the rate and extent of encapsidation were influenced by the CP concentration, the standard 24:1 ratio was compared to reactions where the CP was doubled (CP:RNA ratio of 48:1). With the increased CP levels, no change in the absorbance kinetics was observed for either scaffold tested (TMV genomic RNA or SFV β-gal) (Fig. 3A) indicating that the rate of CP addition to the RNA was independent of CP

Table 1
Tobacco mosaic virus coat protein fusions and peptides employed

Designation	Description	Unprocessed sequence	Molecular weight (Da)	
			Theoretical	Actual
U1	Wild-type TMV U1	M SYS...WTSGPAT	17535.6 (a)	17534
RGD	Integrin receptor fusion	M SYS...WTS AGSGRGDSGA GPAT	18425.5 (a)	18427.3
LSB 1295.10/K TMV	Lysine modified TMV	M EPMK SYS...WTSGPAT	18151.4 (b)	18151.6
Designation	Description	Linker/peptide data	Molecular weight (Da)	
			Theoretical	Actual
SPDP K TMV	SPDP loaded K TMV	Reacted SPDP MW (c) 202 Da or 311 Da	18353.5	18343.9
			18462.5	18453.7
β-gal K TMV	β-gal peptide loaded K TMV	β-gal peptide MW ICPMYARV: 952 Da	19303.7	19297.8

(a) For TMV U1 and TMV RGD, the N-terminal methionine was cleaved and the adjacent serine acetylated. (b) For LSB 1295.10, the N-terminal methionine was retained and acetylated. (c) When reacted with lysine, the MW of the sulfo LC SPDP is dependent on whether the pyridine ring protecting the sulfhydryl group is present (311 Da) or not (202 Da).

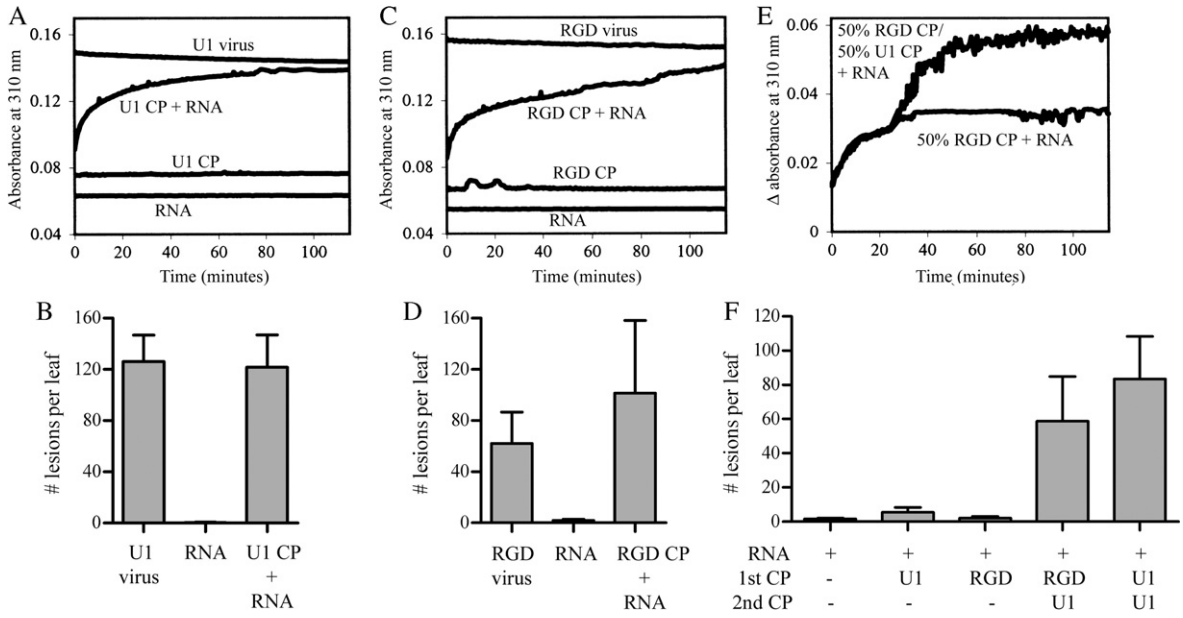

Fig. 2. Single and dual CP reassembly onto TMV genomic RNA. Reassembly over time was monitored by the change in absorbance at 310 nm and functionality of the reassembly product was evaluated by the local lesion assay. (A/B) Reassembly with wild-type U1 CP at a 1:24 RNA to CP mass ratio. (C/D) Reassembly with RGD CP at a 1:24 RNA to CP mass ratio. (E/F) Reassembly of two unique TMV CPs onto a single RNA scaffold in a staged format. TMV genomic RNA was combined with the RGD CP at a mass ratio of 1:10 (50% requirement for encapsidation) and following a 30-min incubation an equal quantity of wild-type U1 CP or buffer was added. For the ordinate, the OD for the CP alone controls was subtracted from the corresponding reassembly OD profile. Legend; RNA, genomic RNA alone; virus, TMV at the same molar concentration as the genomic RNA in the reassembly reactions; CP, coat protein. For the local lesion assay, the mean and standard deviation for 3 leaf inoculations are reported.

concentration. However, since absorbance is proportional to average rod length, the final OD_{310} at which the SFV β-gal transcript plateaued was greater than for the 6.4 kb TMV genomic RNA. In the case of TMV reconstitution, rod elongation was essentially complete after 90 min and the absorbance remained constant thereafter. For the SFV β-gal transcript, the absorbance continued to increase and after 3 h had not yet reached its plateau. For vaccine preparation, encapsidations were therefore left overnight (~16 h) to permit capsid formation to reach completion. The size difference between the two RNA scaffolds was readily evident by TPE agarose gel electrophoresis (Fig. 3B), with TMV U1 virion used as the reference. TMV migrated as a doublet, consisting of a prominent well-defined band (*) and a less intense upper band (**), likely representing virus particles associated end-to-end. Virus reconstituted from TMV genomic RNA and U1 CP co-migrated with the TMV U1 control, while pseudovirus generated by the combination of SFV β-gal transcript with U1 CP formed a distinct band that migrated just below the presumed end-to-end rod band in the TMV U1 control. No band was present when either the CP or RNA scaffold alone was analyzed.

A prerequisite for the use of recombinant TMV CP for the encapsidation of Oa-containing RNA is the ability to isolate reassembly competent CP from purified virus, which is free from RNA contamination. Our experience with over 10 different CP fusions indicated that certain epitopes were incompatible with CP isolation by the acetic acid procedure (Fraenkel-Conrat, 1957). TMV CP has a characteristic UV absorption profile, with a reported maximum to minimum absorbance ratio of 2.5 or greater (Fraenkel-Conrat, 1957). In our hands, wild-type U1 CP had an absorbance ratio of 2.2–2.4 and for the CP fusions listed in Table 1 and successfully employed for transcript encapsidation (Figs. 1–3), the ratio was 2.0 or greater. CPs that failed to reassemble had ratios of 1.0 to 1.8 suggestive of RNA contamination. Alternative chromatographic procedures developed to separate the CP from RNA (Durham, 1972) were considered, but these either gave poor recoveries or were ineffective as the CP elution characteristics were altered by the epitope displayed (data not shown). Furthermore for certain epitopes, CP with the desired absorbance ratio was recovered but aggregated and precipitated when adjusted to 0.1 M phosphate for reassembly.

Since the display of epitopes on the pseudovirion surface as genetic fusions may be limited by the ability to isolate the recombinant CP, chemical conjugation of peptides to the surface of reassembly products was also considered. For this approach, LSB 1295.10 CP, which has a single surface exposed lysine (Smith et al., 2006) and is capable of self-assembly, was employed. A $CD8^+$ epitope of β-gal (Oukka et al., 1996) was conjugated to pseudovirions composed of TMV RNA or SFV β-gal RNA encapsidated with LSB 1295.10 CP (Fig. 4). The reassembly product was initially reacted with SPDP and mass spectrometry confirmed reaction with essentially all the CP residues (Fig. 4A) with the expected mass increase obtained (Table 1). Peptide was then added to the activated recombinant TMV or pseudovirion for loading via a disulfide bridge and the extent of peptide loading assessed by protein gel electrophoresis. Relative to the starting CP, β-gal peptide addition reduced the amount of pseudovirus monomer (arrow) by approximately

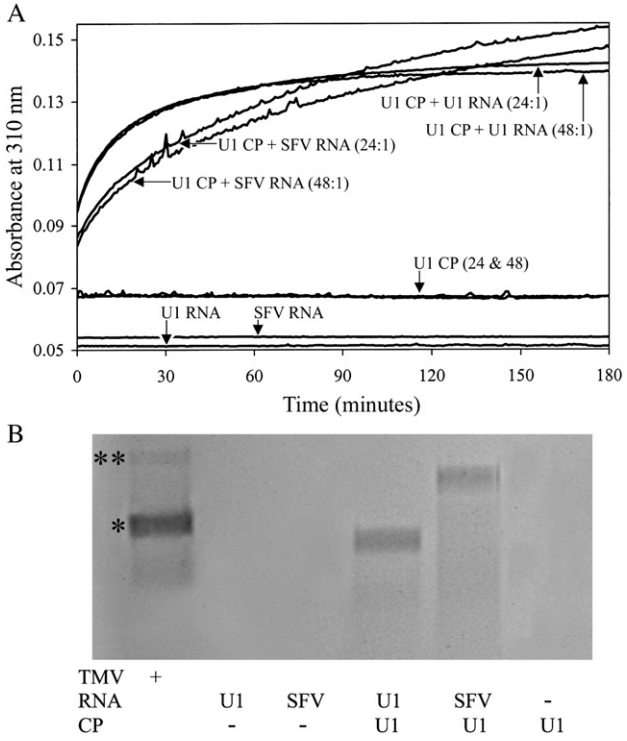

Fig. 3. Characterization of TMV CP reassembly onto Oa-containing RNA scaffolds. (A) Comparison of the reassembly OD 310 nm kinetic profiles for wild-type U1 CP combined with TMV genomic RNA or SFV β-gal transcript. Both RNA scaffolds were employed at the same mass concentration and the CP was added at either a 24-fold or 48-fold mass excess. (B) Comparison of the migration rates for reassembly products generated from the 24:1 mass ratio CP: RNA combinations in panel A on Coomassie-stained 0.5% TPE agarose gels, relative to the migration of TMV U1. *, TMV virion band, **, putative TMV rods associated end-to-end.

50%, as determined by densitometry (Fig. 4B). A weak band (*) corresponding to the addition of a single peptide was detected, the identity of which was confirmed by MALDI-Tof (Fig. 4C and Table 1). The majority of the conjugated species migrated as a putative CP dimer (**), although the mechanism of dimer formation was unclear.

In vitro testing of the SFV β-gal/TMV CP encapsidated pseudovirus particles

The functionality of the pseudovirus particles was initially tested *in vitro* using BioTrek-mediated uptake in baby hamster kidney (BHK21) cells. After 24 h, expression of β-galactosidase was observed (Figs. 5A and B), demonstrating that following facilitated uptake by the cells the pseudovirion was effectively uncoated, replicated and the reporter gene translated. To confirm that naked transcript, which may have been present in the encapsidated SFV β-gal preparations was not responsible for the observed staining, cells were also incubated with RNA alone. No significant β-gal staining in these negative controls was observed, even when the transcript was present in a 10-fold excess relative to the amount of experimental encapsidated SFV β-gal RNA (Fig. 5C). This result indicates that only TMV CP encapsidated SFV β-gal was translocated into the cells. For *in vivo* studies, encapsidated transcript was prepared and stored at −20 °C, with aliquots removed for each of the immunizations. To confirm that the pseudovirions remained functional after −20 °C storage, we performed a stability study over a 3-month period, by incubating thawed aliquots with BHK21 cells and staining for β-gal activity (Fig. 5D). An approximately equivalent number of cells were positive for β-gal protein expression indicating that no decline in potency occurred with storage. Testing was also performed with 1295.10 CP-encapsidated pseudovirus decorated with peptide (ICPMYARV; Table 1). The level of staining was unaffected (data not shown), indicating that SPDP conjugation and peptide loading did not alter the disassembly and transcription properties of the vector.

Comparison of U1 CP and RGD CP encapsidated SFV β-gal in vivo

To determine the ability of encapsidated SFV β-gal RNA to elicit immune response, we encapsidated SFV β-gal RNA with either the U1 or RGD CPs. A 20 μg unadjuvanted dose of pseudovirus (1 μg SFV β-gal RNA) was administered, with serum samples taken following the third and fourth

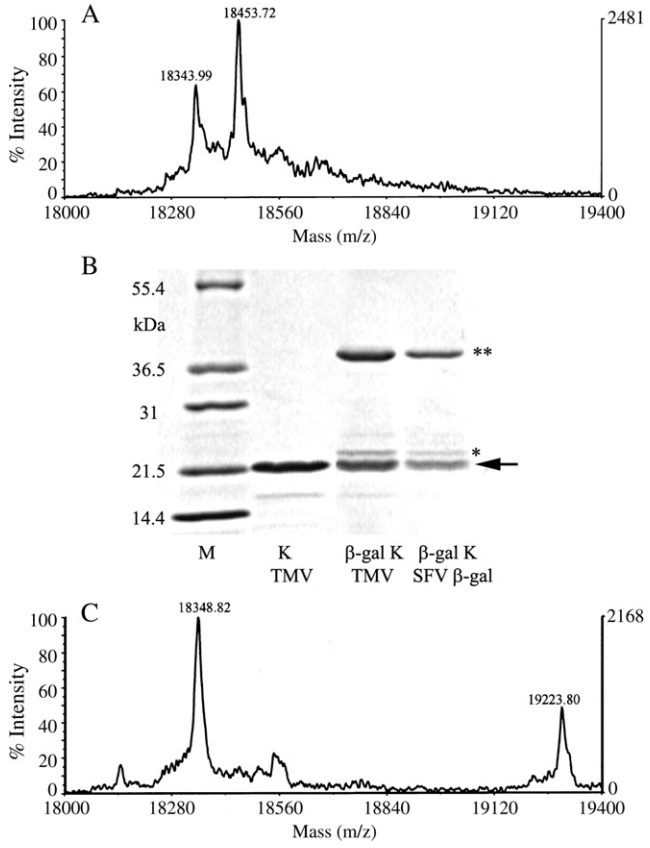

Fig. 4. Peptide conjugation to lysine-modified TMV CP capsids. (A) MALDI-Tof spectra for heterobifunctional linker SPDP conjugated 1295.10 CP. SPDP increases CP mass by 313.1 or 203.2 Da (see Table 1) (B) SDS-PAGE analysis for the conjugation of a cysteine containing β-gal derived peptide (β-gal) to 1295.10 virus (K TMV) or 1295.10 CP encapsidated SFV β-gal transcript (K SFV β-gal) via the SPDP linker. Arrow, indicates the CP monomer band; *, peptide loaded CP monomer; **, CP dimer. (C) MALDI-Tof spectra for peptide addition to SPDP activated LSB 1295.10 CP (see Table 1).

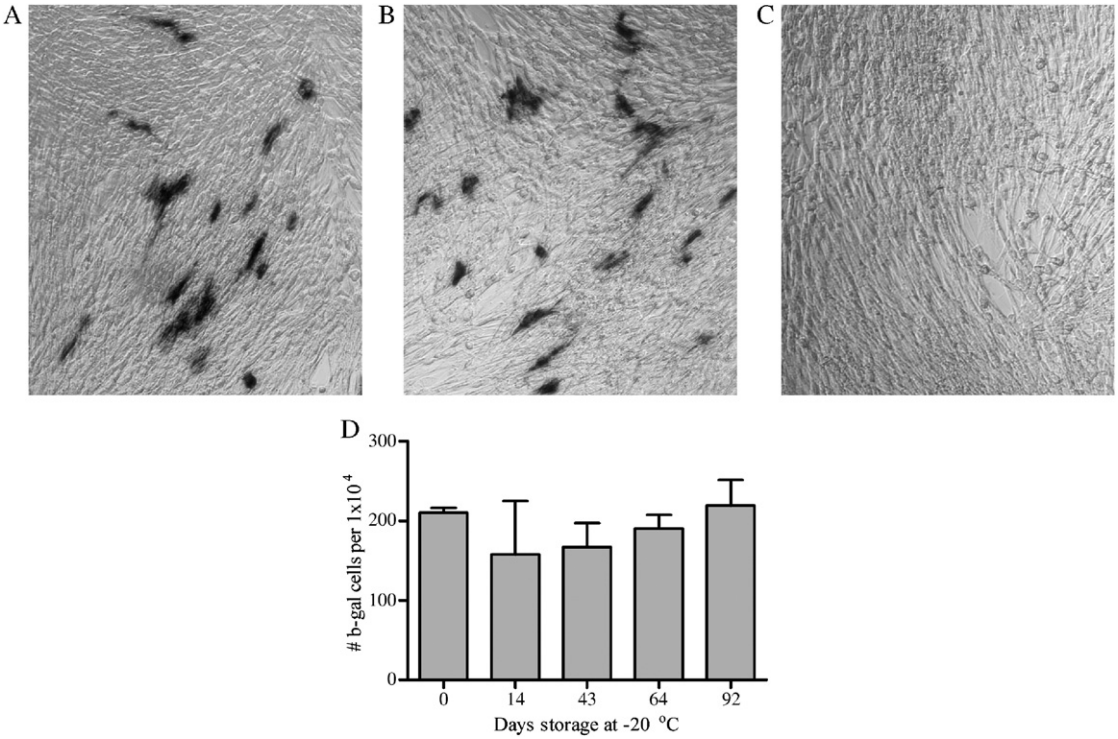

Fig. 5. Evaluation of TMV CP encapsidated SFV β-gal vector functionality and stability *in vitro*. Encapsidated transcript or RNA alone was combined with the protein translocation reagent BioTrek and incubated with BHK-21 cells that were subsequently stained for β-gal activity. (A) 25 ng SFV β-gal transcript encapsidated with U1 CP (0.5 μg reassembly product on a protein basis). (B) 100 ng SFV β-gal transcript encapsidated with 1295.10 CP (2 μg of reassembly product on a protein basis). (C) Negative control; 1000 ng of unencapsidated SFV β-gal transcript. (D) Stability testing of 1295.10 CP encapsidated SFV β-gal transcript with storage at −20 °C. Mean and standard deviation for 6 replicate wells at each timepoint are reported.

immunizations. For pseudovirion with a U1 CP capsid, antibodies against β-galactosidase were detected following the fourth immunization although levels were 100–1000 fold lower than the average response observed in mice that received 25 μg doses of β-gal protein (Fig. 6A). In contrast to pseudovirion, administration of 1 μg naked SFV β-gal RNA failed to elicit a measurable response and this was also the case for repeated immunization with 100 μg plasmid DNA. When the U1 CP was replaced with the RGD CP, no significant improvement in the humoral immune response was observed (data not shown). One animal from each group was immunized a fifth time and after 5 days we evaluated T-cell responses by IFNγ ELIspot. As shown in Fig. 6B, animals immunized with the DNA plasmid or the encapsidated SFV β-gal transcript showed a significant T-cell activation response, while no response was observed after β-gal protein immunization. Fig. 6B also suggested that there was limited benefit, in terms of T-cell activation, to encapsidation with the RGD CP. Based on this and the humoral response data, evaluation of the RGD CP *in vivo* was not pursued further.

Ability of encapsidated SFV β-gal to prime β-gal protein immunization

Next, we tested the ability of pre-immunization (or priming) with SFV β-gal to boost the immune response to a single dose of β-gal protein (Table 2). With a single pseudovirion prime (Fig. 7A; groups 2-2 and 2-4), only animals receiving pseudovirion 2 weeks prior to the protein boost had significant antibody titers (group 2-4) relative to the PBS control (group 2-1), while a naked RNA prime was ineffective (groups 2-5 and 2-6). Therefore, both priming schedule and encapsidation of the RNA transcript were critical for a humoral response. With the administration of pseudovirion twice (group 2-3), the mean antibody titer was increased 50-fold relative to the single immunization. Cellular responses were also measured in two mice per group 10 days after the protein boost (Fig. 7B). Only animals receiving two doses of pseudovirion prior to the β-gal boost (group 2-3) showed a statistically significant response relative to the control (group 2-1).

Immunogenicity of SFV β-gal pseudovirion displaying a β-gal CTL peptide

Encapsidation of SFV β-gal by LSB 1295.10 CP permits the display of proteins or peptides on the capsid surface through chemical conjugation (Fig. 4) that could potentially modulate and/or augment the immune response elicited by the RNA. Rather than a prime-boost regime, with RNA and protein administered separately, we evaluated pseudovirion with a CD8+ CTL peptide conjugated to the TMV CP, which should boost the same Kb restricted β-gal peptide encoded by the encapsidated SFV vector (Table 3; groups 3-5 and 3-6). To distinguish between contributions from the RNA and conjugated peptide to the humoral and cellular immune responses, pseudovirion lacking peptide (groups 3-3 and 3-4) and peptide conjugated to

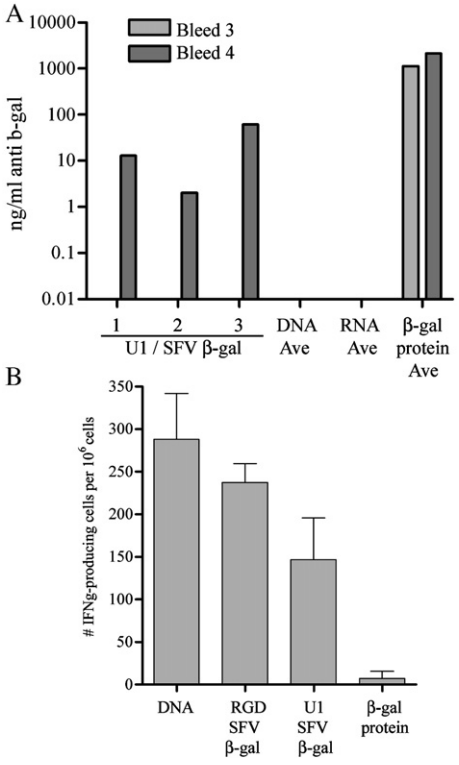

Fig. 6. Humoral and cellular immune responses to the SFV β-gal transcript encapsidated with either U1 or RGD CP. Groups of five mice were employed and the high and low responders from each group were omitted for the humoral response analysis. (A) Antibody response against β-galactosidase, for animals administered 20 μg U1 CP encapsidated SFV β-gal transcript (U1/SFV β-gal; 1000 ng RNA). The average responses (Ave) for the groups receiving DNA (100 μg), RNA transcript alone (1000 ng) or β-galactosidase protein (25 μg) are also plotted. (B) Comparison of IFNg response following peptide stimulation. Mean and standard deviation for 12 replicate wells for each group are reported. The SFV β-gal RNA encapsidated with RGD CP (RGD/SFV β-gal) was administered at 20 μg protein per dose.

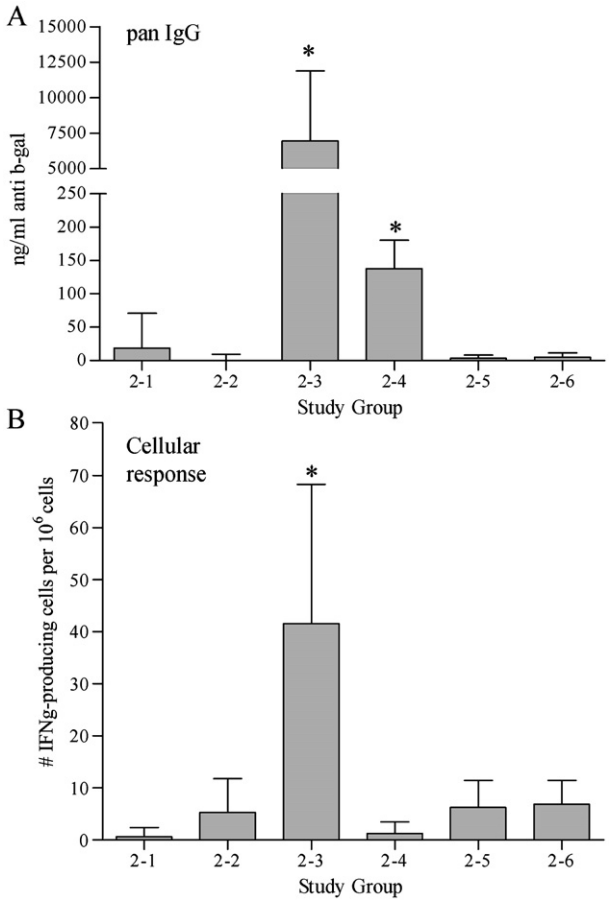

Fig. 7. Humoral and cellular immune responses for TMV U1 CP encapsidated SFV β-gal transcript employed in a prime/boost regime with β-galactosidase protein. The vaccine schedules for each group are summarized in Table 2. (A) Anti-β-galactosidase response in bleeds taken 8 days following the final immunization. Groups of five mice were employed and the high and low responders from each group were omitted in the analysis. Averages and standard deviations for each group are plotted. *, indicates the average response was statistically different from group 1; $p \leq 0.0476$. (B) T-cell responses observed with each immunization schedule. Following the final immunization, spleen cells were harvested from two animals in each group and ELIspot analysis performed. Mean and standard deviation for 12 replicate wells for each group are reported. *, indicates the average response was statistically different from group 1; $p < 0.0001$.

LSB 1295.10 virus (groups 3-1 and 3-2) were administered as controls. Following the final immunization, pan IgG and IgG_2 antibody titers were measured to assess the overall humoral immune response and the prevalence of Th1 type T-help during B-cell stimulation (Figs. 8A and B). As expected, β-gal peptide conjugated to the lysine modified TMV did not elicit antibody titers above background levels (PBS immunization; group 3-8), as the epitope displayed was a T-cell activation target. For the SFV β-gal pseudovirus, pan IgG was detectable with two immunizations and a strong IgG_2 response was also observed, suggesting active T-help. However, unexpectedly, when the peptide and RNA components were combined the antibody response was severely blunted following two immunizations and was completely abrogated with administration of the third dose (Fig. 8B, 3.5 and 3.6).

In Fig. 8C, the cellular responses obtained following two immunizations are compared. The peptide conjugated to LSB 1295.10 TMV elicited significant levels of T-cell activation, with approximately 600 per 10^6 IFNγ secreting cells detected (group 3-1). In contrast the level of T-cell activation obtained with encapsidated SFV β-gal was approximately 7-fold lower

Table 2
Study design for the evaluation of SFV β-gal RNA in an encapsidated vector prime/protein boost schedule

Group	Immunization schedule			# mice/ group
	#1	#2	#3	
2-1	PBS	PBS	25 μg β-gal protein	5
2-2	20 μg U1/SFV β-gal	–	25 μg β-gal protein	5
2-3	20 μg U1/SFV β-gal	20 μg U1/SFV β-gal	25 μg β-gal protein	5
2-4	–	20 μg U1/SFV β-gal	25 μg β-gal protein	5
2-5	1 μg SFV β-gal	–	25 μg β-gal protein	5
2-6	–	1 μg SFV β-gal	25 μg β-gal protein	5

U1/SFV β-gal, U1 coat protein encapsidated transcript; SFV β-gal, transcript alone.

Table 3
Study design to evaluate the immunogenicity of encapsidated SFV b-gal transcript decorated with a T-cell restricted β-gal peptide

Group	Antigen dose and composition			Immunization schedule			# mice/ group
	TMV	Encapsidated transcript/transcript		#1	#2	#3	
		CP	RNA				
3-1	25 μg β-gal K	–	–		x	x	4
3-2	25 μg β-gal K	–	–	x	x	x	3
3-3	–	25 μg K	SFV β-gal ET		x	x	4
3-4	–	25 μg K	SFV β-gal ET	x	x	x	3
3-5	–	25 μg β-gal K	SFV β-gal ET		x	x	4
3-6	–	25 μg β-gal K	SFV β-gal ET	x	x	x	3
3-7	–	–	10 μg SFV β-gal	x	x	x	3
3-8	PBS	–	–	x	x	x	3

β-gal K, β-gal peptide decorated LSB 1295.10 CP or TMV; SFV β-gal, RNA transcript; K, LSB 1295.10 CP; ET, encapsidated transcript. Immunization schedule; x indicates dose administration.

(group 3-3) and comparable to previously observed results (Figs. 6 and 7). Decoration of the SFV β-gal capsid with peptide augmented the cellular response by approximately 50% relative to peptide alone (group 3-5) and the increase observed was statistically greater than the individual peptide and RNA contributions (3.1+3.3; theoretical value). With the third immunization, this differentiation was not maintained and the responses to the peptide with and without SFV β-gal were comparable (data not shown). In parallel with the bifunctional pseudovirus testing, a high dose RNA immunization schedule was also evaluated (group 3-7). SFV β-gal RNA was administered at a 10 μg dose, 10-fold higher than previously tested, in order to determine the extent of the immunological response elicited by unencapsidated RNA vector alone. At the higher dose, we observed both humoral and cellular immune responses following three immunizations (Fig. 8A, group 3-7; Fig. 8D). However, the mean antibody titers were 2–4-fold lower and T-cell activation 2-fold lower relative to immunization with the encapsidated SFV β-gal (group 3-4), where transcript dose was 1.25 μg. Therefore, encapsidation of RNA improved vector efficiency, as measured by increased levels of humoral and cellular immune responses to SFV-produced protein, while permitting transcript dose to be reduced by at least 8-fold.

Discussion

To our knowledge, this is the first demonstration *in vivo* of the uptake and replication of a plant virus CP-encapsidated animal RNA virus vector. The ability to efficiently encapsidate RNAs of interest with a plant virus CP could offer a safer alternative to current animal RNA virus encapsidation strategies. The CP of TMV can accept small (generally up to 25 amino acid) peptide fusions with multiple reports showing the utility of TMV in vaccine applications, through the display of neutralizing epitopes (reviewed in Pogue et al., 2002). Recently we described a methodology for the display of whole proteins on the surface of TMV (Smith et al., 2006) and have also shown that TMV displaying T-cell epitopes can elicit a strong cellular immune response, capable of protecting mice against tumor challenge (McCormick et al., 2006). Disassociating the recombinant TMV particles and isolating free, reassembly competent CP, which either displays an immunologically relevant peptide or has been modified to accept peptides/proteins via chemical conjugation opens the possibility of generating bifunctional pseudovirions composed of complementary protein and nucleic acid components. Employing both wild-type and recombinant CPs, the successful encapsidation of the 13.6 kb TMV Oa SFV β-gal transcript was confirmed by electron microscopy (Fig. 1) and the kinetics of reassembly compared with TMV genomic RNA as the scaffold (Fig. 3). To demonstrate dual CP virion formation, sequential CP addition to the RNA transcript was performed and we were able to observe the staged addition of the capsid by the OD_{310} as well as the recovery of infectivity by the local lesion assay (Figs. 2E and F). From electron micrographs, an estimated 35% of the bivalent encapsidated pseudovirus were full length (data not shown) indicating further optimization to improve yield is possible. We were also able to obtain pseudovirions with tailored surface compositions by mixing two CP preparation before the addition of the RNA scaffold (data not shown).

To evaluate improved cellular uptake with the RGD CP fusion, SFV β-gal encapsidated transcripts were incubated with BHK21 cells, which express integrin $\alpha_v\beta_3$, the receptor for the RGD cell-binding motif (Alcala et al., 2001). However, testing in the absence of the BioTrek protein translocation reagent showed no intracellular β-gal expression (data not shown), indicating no measurable pseudovirion internalization. One possibility is that particle size may play a role. RGD has been employed successfully in the context of soluble proteins (Alcala et al., 2001) and icosahedral capsids (Magnusson et al., 2001) with diameters less than 100 nm, whereas the rod-like SFV β-gal capsids were approximately 600 nm in length and possibly too large to facilitate receptor meditated uptake. However, once internalized with the aid of the BioTrek reagent, reporter gene expression was obtained, demonstrating that a plant CP capsid can be efficiently disassembled within a mammalian cell to allow RNA replication and translation (Fig. 5). Furthermore, the SFV β-gal encapsidated by U1 CP was immunogenic (Figs. 6–8) and therefore successfully internalized and processed by immune effector cells. The humoral (data not shown) and cellular immune responses (Fig. 6B) elicited by RGD CP packaged transcript were comparable to U1 CP encapsidation,

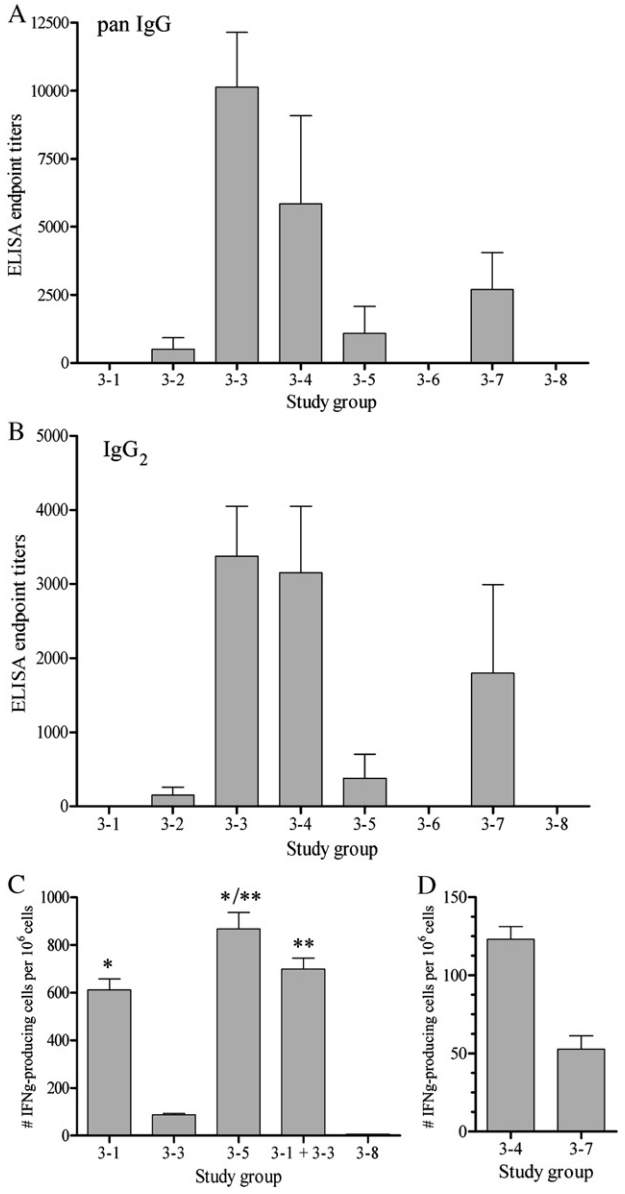

Fig. 8. Humoral and cellular immune responses for encapsidated SFV β-gal transcript decorated with a β-gal derived CTL epitope. The experimental design and group designations are outlined in Table 3. (A and B) Pan IgG and IgG_2 serum antibody responses against β-galactosidase 8 days following the final immunization. Averages and standard deviations for each group are plotted. (C) T-cell responses observed in the subset of groups that received two immunizations. Following the final immunization, spleen cells were harvested from 4 animals in the selected groups and ELIspot analysis performed. *, response in group 3-5 was statistically different from group 3-1; $p=0.0026$. **, response in group 3-5 was statistically different from the theoretical sum of the responses from groups 3-1 and 3-3; $p=0.042$. (D) Comparison of T-cell response after three immunizations for the 10 μg transcript dose (3–7) with the response obtained from 8-fold less encapsidated transcript (3–4). For the ELIspot analysis, mean and standard deviation for 12 replicate wells for each group are reported.

indicating that for the pseudovirions considered in this study, uptake by phagocytic and/or endocytic mechanisms was sufficient and obviated the need for cell fusion motifs. This *in vivo* data are in agreement with our previous observation of spontaneous and efficient wild-type U1 TMV uptake by either isolated spleen or bone marrow cells (McCormick et al., 2006).

When immunization with SFV β-gal alone was compared to encapsidated transcript administered at equivalent nucleic acid doses (Figs. 6 and 7), encapsidated transcript repeatedly produced superior humoral immune responses, with no anti-β-gal detected in the sera of animals vaccinated with RNA alone. By increasing the free transcript dose, cellular and humoral immune responses were obtained (Fig. 8); however, both antibody titers and activated CD8+ T-cell numbers were notably higher with a significantly lower dose of encapsidated SFV β-gal, indicating that particulate antigen uptake is an effective mechanism for RNA vector delivery. These results are consistent with those from several groups that have directly compared transcript with recombinant SFV particles (Andersson et al., 2001; Berglund et al., 1999; Brand et al., 1998; Fleeton et al., 2000; Zhou et al., 1994, 1995). It would therefore be interesting to compare the pseudovirions created in this study with the SFV transcript encapsidated by its native CP, to evaluate how a heterologous CP impacts nucleic acid potency. In addition, it would be informative to compare, through histochemical staining, the localization of the TMV CP-encapsidated vector with that of recombinant SFV particles (Morris-Downes et al., 2001) and naked SFV RNA. Formative early studies in rabbits demonstrated that owing to their particulate structure, ^{14}C-labeled TMV virions were rapidly and effectively transported from the site of injection to proximal lymph nodes, and then to the spleen (Loor, 1967).

At a dose of 1000 ng naked transcript, we were unable to obtain T-cell activation. In contrast, others have reported that as little as a single 100 ng RNA dose successfully elicited a CD8+ T-cell response (Ying et al., 1999). Ying et al. employed a similar vector (lacking the Oa); however, the mouse strain/restricted peptide combination (Balb/C/β-$gal_{876–884}$ LPYLGWLVF) was different to the current study and peptide restimulation prior to IFNγ measurement was for 6 days, while we employed a 22-h stimulation, which limits the augmentation of the response by cell proliferation. Genetic immunizations typically generate low levels of antibodies, with more robust T-cell responses due to intracellular expression and processing of the antigen. With DNA immunization, appropriate class I peptide loading did occur and was confirmed by the detection of activated IFNγ secreting CD8+ T-cells following β-gal peptide stimulation (Fig. 6B). No humoral immune response was observed, even with the 100 μg dose; however, this may reflect the antigen expressed (β-gal) rather than the mode of vaccination itself, since we have employed a similar DNA vaccine expressing green fluorescent protein and obtained an antibody response in mice (data not shown). In the case of encapsidated SFV β-gal, antibodies were detected, most likely due to β-gal escape from cells expressing the reporter gene that had undergone apoptosis and lysis (Ying et al., 1999). As expected, titers were significantly lower than in animals immunized with β-gal protein (Fig. 6A) indicating that effective priming was obtained, but boosting was low due to reduced protein concentrations. In an attempt to augment the immune response, we complemented the nucleic acid prime with a single β-gal protein boost (Fig. 7)

a strategy that has previously been shown to be effective (Sin et al., 1999; Soleimanjahi et al., 2006). We observed that effective priming required the SFV β-gal to be encapsidated and that the timing of the protein boost was also an important factor. By priming twice with the encapsidated transcript, we were able to further improve the humoral response and also elicit a CD8+ T-cell response. Overall, similar to previous studies that demonstrate upregulation of both antibody and cellular responses with nucleic acid priming and protein boosting, we also see marked increases in both types of immune responses when encapsidated SFV β-gal was employed.

One of the recombinant CPs proteins employed, LSB 1295.10, was engineered with a surface exposed N-terminal lysine. Lysine is compatible with numerous commercially available linkers permitting the co-delivery of proteins or peptides with the encapsidated transcript. In the present study, a β-gal CTL restricted peptide was combined with the β-gal nucleic acid signal encoded by encapsidated SFV RNA to generate a bifunctional pseudovirion (Fig. 8). We hypothesized that inclusion of a surface fused peptide would provide complementary protein boosting and improve T-cell activation over that generated from RNA transcript alone. When a β-gal peptide fused to TMV was administered, potent T-cell activation was observed, and the response was notably superior to encapsidated β-gal RNA. T-cell stimulation was improved still further with the bifunctional pseudovirion and the response observed was significantly greater than the theoretical combined value for the peptide and the RNA given as single agents (Fig. 8C). The superior T-cell response obtained with the conjugate vaccine relative to pseudovirion suggests that the quantity of peptide delivered via CP unloading may exceed that generated by RNA translation and subsequent β-gal proteolysis. Alternatively, the conjugate vaccine may deliver peptide antigen more rapidly, resulting in better antigen presentation to dendritic cells as compared to long-term low-level antigen delivery by RNA translation.

An unexpected consequence of the bifunctional pseudovirions was a downregulation of the humoral immune response, with no circulating β-gal specific antibodies detected after three immunizations. Animals receiving the encapsidated transcript lacking peptide showed good humoral responses suggesting that the potent stimulatory properties of the peptide may have skewed the immune response to T-cell activation. For some vaccine strategies, a highly desirable outcome is the control the Th1/Th2 response to immunization. For example, an early formalin-inactivated vaccine composition for the prevention of respiratory syncitial virus induced a Th2-type antibody response that exacerbated disease characteristics in some children, and was subsequently withdrawn (reviewed in Piedra, 2003).

In summary, these data support the observation that encapsidated RNA can augment antigen-specific immune responses, and this concept will be explored further in ongoing studies. The ability of this system to present both peptide antigens and intact proteins through a combination of CP fusion and SFV vector expression provides for flexibility in vaccine design. Through both genetic fusion and chemical conjugation, one or multiple antigens can decorate the pseudovirion capsid, and the response to these surface displayed immunogens can be enhanced and/or skewed by the co-expression of the same antigen (as presented here), or by expression of immunomodulatory proteins such as cytokines from the SFV replicon. With regard to the potential for scale-up, we have successfully modified the original coat protein isolation procedure (Fraenkel-Conrat, 1957) to isolate up to 6 g of reassembly competent coat protein on a laboratory scale, and believe that further scale-up is possible. In parallel, improved processes are being developed for large-scale capped RNAs synthesis, including batch-fed methodologies that increase the yield of RNA synthesis by 5- to 6-fold under current Good Manufacturing Practices (cGMP; Emmanuel Labourier, Asuragen Inc., personal communication). Linking best-mode technologies will support the further development of this new vaccine platform.

Materials and methods

RNA scaffold vector construction

The SFV β-gal vector (Fig. 1B) was generated by introducing the TMV origin of assembly (Oa) 3′ of the lacZ gene in the pSFV3-lacZ vector (Invitrogen, Carlsbad, CA). The TMV Oa was amplified by PCR from plasmid p801 (Dawson et al., 1986), containing the full length cDNA of TMV U1, by standard techniques. The resulting PCR product of about 315 bp was digested with *Xma*I and ligated into *Xma*I digested pSFV3-lacZ. Clones with the correctly oriented TMV Oa fragment were identified by sequencing. To obtain SFV β-gal transcript, the *Spe*I linearized vector was purified using a Zymo-spin column (Zymo Research Corporation, Orange, CA) and transcribed with SP6 RNA polymerase using the SP6 mMessage mMachine kit (Ambion, Austin, TX), according to the manufacturer's instructions. The RNA was isopropanol precipitated prior to encapsidation. For instances where TMV genomic RNA was used as the scaffold, the RNA was isolated from purified wild-type U1 TMV using a Qiagen RNeasy kit (Valencia, CA).

Cloning, expression and purification of the TMV coat protein fusions

The amino and carboxy termini of the TMV CP reside on the exterior of the TMV capsid, allowing amino acid fusions in either location to be displayed on the virion surface. A series of lysine-modified TMVs were generated (Smith et al., 2006) and from this series LSB 1295.10 (Table 1) was selected based on the level of SPDP conjugation obtained, relative to the other constructs evaluated (data not shown). For the TMV CP fusion displaying the integrin fusion receptor (Magnusson et al., 2001), standard molecular techniques were used to fuse the amino acid sequence SGRGDSG to the 3′ end of the TMV CP ORF, in a plasmid containing the full-length cDNA clone of TMV RNA, under the control of the T7 RNA polymerase promoter. The RGD peptide was located 4 amino acid from the native carboxy terminus and bounded by the linker amino acids AG and A that were introduced by the cloning strategy used (Table 1; RGD). Infectious transcripts of each clone were generated with T7 polymerase from the respective DNA plasmid, using the

Message mMachine kit (Ambion), according to the manufacturer's instructions. *Nicotiana benthamiana* plants were inoculated and recombinant TMV purified from systemically infected *N. benthamiana* as previously described (Smith et al., 2006). In the case of wild-type TMV U1, previously isolated virion was employed as inoculum and *Nicotiana tabacum* (cv. MD609) replaced *N. benthamiana* as the host.

Analytical procedures, immunoassays and electron microscopy

Polyacrylamide gel electrophoresis (PAGE) was performed on 10–20% Tris glycine gels (Invitrogen), following the manufacturer's instructions. For gel analysis by densitometry, a GS810 calibrated densitometer in conjunction with the Quantity 1 software (both BioRad) was used. The Mark 12 protein standard (Invitrogen) was employed as molecular weight reference. Encapsidated transcripts were analyzed by Tris/Phosphate/EDTA (TPE) agarose gel electrophoresis (Sambrook et al., 1989). Samples were resuspended in DNA gel loading dye (Promega, Madison, WI) and electrophoresis was performed at 150 mA for 2–3 h, with the 0.5% w/v agarose gels and buffer chilled to 4 °C prior to use. Agarose gels were stained overnight in 10% v/v glacial acetic acid/40% v/v ethanol containing 0.1% w/v Coomassie brilliant blue R-250 and destained using the same buffer lacking dye. Protein quantitation was performed using the bicinchoninic acid (BCA) assay (Pierce, Rockford, IL) in a microtiter plate format following the manufacturer's instructions. Protein mass determination was performed by matrix-assisted laser desorption ionization time-of-flight mass spectrometry (MALDI-TOF MS). The increase in infectivity, following encapsidation, for reassembly reactions that employed TMV genomic RNA as a scaffold, was evaluated on the local lesion host *N. tabacum* cv. *xanthi* (N). For electron microscopy, grids (400 Mesh copper, carbon coated; Ted Pella, Bedding, CA) were floated on drops of encapsidated transcript and negatively stained with 1% phosphotungstic acid. The MALDI-TOF MS, local lesion assay and electron microscopy grid preparation are described in greater detail elsewhere (Smith et al., 2006).

Preparation of free TMV coat protein

The wild-type or recombinant virus preparations were diluted to 1 mg/ml and treated with powdered activated carbon (Norit, Marshall, TX) at 1% w/v with stirring for 1 h at 4 °C. Following centrifugation (10,000×*g* for 10 min) to remove the activated carbon, the virus was concentrated to 10–20 mg/ml by PEG precipitation, prior to virus disassociation by acetic acid (Fraenkel-Conrat, 1957). CP preparations were stored at 4 °C in the presence of 0.02% w/v sodium azide and were confirmed RNA free when no local lesions were detected following inoculation onto the local lesion host at a minimum protein concentration of 2 mg/ml.

Reassembly of TMV coat protein onto Oa-containing RNA scaffolds

In reassembly reactions, the RNA scaffold and CP were combined at a mass ratio of 1:24 or 1:48, the former ratio corresponding to a 30% molar excess of CP. Final RNA and CP concentrations were confirmed by gel electrophoresis for both the reassembly reactions and controls. During encapsidation, appropriate precautions were taken to ensure that all buffers and labware were ribonuclease-free. Prior to use, the CP was dialyzed against 0.1 M phosphate pH 7.0 at 4 °C, centrifuged at 20,000×*g* for 30 min to remove any precipitate that formed and pre-equilibrated for 36 to 48 h at room temperature, to permit 20 S disk formation (Durham and Klug, 1971). The RNA scaffold was diluted in phosphate buffer to a final buffer molarity of 0.1 M and the equilibrated CP added to give a final RNA concentration of 50 μg/ml. The reassembly reactions were allowed to proceed for 3–4 h (TMV genomic) or overnight (SFV β-gal transcript) and when required, the encapsidation products recovered by 4% w/v PEG precipitation in the presence of 4% w/v NaCl. To monitor the reassembly process by absorbance at 310 nm (Butler and Klug, 1971), the reactions and controls were placed in a 96-well polystyrene plate (Nalge Nunc, Rochester, NY) and the increase in absorbance tracked using a 96-well plate spectrophotometer (Molecular Devices, Sunnyvale, CA).

Chemical conjugation of peptides to lysine modified capsids

Conjugation reactions were performed with purified LSB 1295.10 virion or LSB 1295.10 CP encapsidated SFV β-gal transcript. To permit peptide loading, the virion/encapsidated transcript was combined with a 20-fold molar excess of sulfo LC-SPDP (Pierce) in PBS containing 5 mM EDTA and incubated for 4 h at room temperature. Unreacted heterobifunctioal linker was removed by dialysis and the β-gal peptide (ICPMYARV) added at a 10-fold molar excess. The conjugation reactions were incubated with end-to-end rotation at room temperature, for 16 h. Free peptide was removed by dialysis and peptide conjugation confirmed by MALDI-TOF MS. The percentage of CP displaying the β-gal peptide was estimated by densitometry for PAGE performed under non-reducing conditions.

In vitro testing of SFV β-gal encapsidated vectors

The functionality of the SFV β-gal encapsidated vectors was evaluated *in vitro*. BHK-21 cells (plated at 2×10^4 cells/well 24 h prior to testing) were incubated with 0.5–2 μg of freshly prepared pseudovirus particles on a protein basis (25–40 ng transcript) combined with the protein translocation reagent BioTrek (Stratagene, La Jolla, CA). After a 3–4-h incubation, the cells were washed and incubated a further 18 h in complete DMEM media with 20% fetal bovine serum. The cells were then washed and stained for beta-galactosidase activity with the X-gal staining kit (Invitrogen). Stained cells were counted using an ELIspot reader (AID, Strassberg, Germany). Free SFV β-gal transcript (0.1–1 μg) was used as a control and samples were tested in replicates of six.

Immunogenicity testing in mice and serological/cellular response analysis

The murine studies were performed using 6–8 week old female C57/b6 mice (Harlan Sprague–Dawley, Indianapolis,

IN) that were housed at Antibodies Inc. (Davis, CA). The reported doses for virion and encapsidated transcript (Tables 2 and 3) are based on protein as quantitated by the BCA assay. The RNA dose per immunization corresponds to approximately 5% of the protein dose. When transcript alone was administered, the reported dose was for RNA alone, as determined by OD_{260}. DNA immunizations employed the plasmid pcDNA3.1/His/LacZ (Invitrogen) that expressed β-gal. Vaccine was administered subcutaneously (s.c.) at 2-week intervals unless otherwise noted and serum samples obtained by tail bleed, 8–10 days post-immunization. The humoral immune response was determined by enzyme linked immunosorbent assay (ELISA) as previously described (Smith et al., 2006) with β-gal protein coated at 5 μg/ml employed as the capture antigen. Anti-β-gal titers reported in ng/ml were determined from a standard curve generated by a 3-fold serial dilution of a 1000 ng/ml mouse anti-β-gal monoclonal antibody (Promega). Serum endpoint dilutions corresponded to an absorbance reading of twice that obtained with pooled sera taken prior to the first immunization.

To evaluate the cellular response, spleens were harvested and single cell suspensions generated. Cell plating on IFNγ antibody coated plates, peptide stimulation, assay development and counting of positive spots were performed as previously described (McCormick et al., 2006). The β-gal derived C57b/6 restricted CTL epitope (ICPMYARV; Oukka et al., 1996) was used for stimulation with an ovalbumin peptide (SIINFEKL; Rotzschke et al., 1991) employed as a control. The peptides (purity >95%) were synthesized by Biomer Technology (Hayward, CA). Data and statistical analysis (unpaired *t*-tests) were performed using GraphPad (version 4.0; San Diego, CA).

Acknowledgments

The authors are grateful to Michael McCulloch for excellent technical assistance and to Dr. Hal Padgett for insightful discussions on the reassembly of multiple recombinant coat proteins onto a single RNA scaffold. The plasmid p801 was a kind gift from Dr. William Dawson, University of Florida. The TMV reassembly image (Fig. 1A) was employed with permission from Dr. Gerald Stubbs. TMV visualization was conducted at the electron microscopy laboratory of the University of California at Davis (UCD) School of Medicine and we thank Grete Admanson for helpful technical advice. This grant was supported by a NIST ATP program grant, # 70NANB2H3048.

References

Alcala, P., Feliu, J.X., Aris, A., Villaverde, A., 2001. Efficient accommodation of recombinant, foot-and-mouth disease virus RGD peptides to cell-surface integrins. Biochem. Biophys. Res. Commun. 285 (2), 201–206.

Andersson, C., Vasconcelos, N.M., Sievertzon, M., Haddad, D., Liljeqvist, S., Berglund, P., Liljestrom, P., Ahlborg, N., Stahl, S., Berzins, K., 2001. Comparative immunization study using RNA and DNA constructs encoding a part of the Plasmodium falciparum antigen Pf332. Scand. J. Immunol. 54 (1–2), 117–124.

Berglund, P., Sjoberg, M., Garoff, H., Atkins, G.J., Sheahan, B.J., Liljestrom, P., 1993. Semliki Forest virus expression system—Production of conditionally infectious recombinant particles. Biotechnology 11 (8), 916–920.

Berglund, P., Fleeton, M.N., Smerdou, C., Liljestrom, P., 1999. Immunization with recombinant Semliki Forest virus induces protection against influenza challenge in mice. Vaccine 17 (5), 497–507.

Brand, D., Lemiale, F., Turbica, I., Buzelay, L., Brunet, S., Barin, F., 1998. Comparative analysis of humoral immune responses to HIV type 1 envelope glycoproteins in mice immunized with a DNA vaccine, recombinant Semliki Forest virus RNA, or recombinant Semliki Forest virus particles. AIDS Res. Hum. Retroviruses 14 (15), 1369–1377.

Butler, P., 1999. Self-assembly of tobacco mosaic virus: the role of an intermediate aggregate in generating both specificity and speed. Philos. Trans., Biol. Sci. 354 (1383), 537–550.

Butler, P., Klug, A., 1971. Assembly of the particle of tobacco mosaic virus from RNA and disks of protein. Nat. New Biol. 229, 47–50.

Dawson, W.O., Beck, D.L., Knorr, D.A., Grantham, G.L., 1986. cDNA cloning of the complete genome of tobacco mosaic-virus and production of infectious transcripts. Proc. Natl. Acad. Sci. U.S.A. 83 (6), 1832–1836.

Dorange, F., Piver, E., Bru, T., Collin, C., Roingeard, P., Pages, J.C., 2004. Vesicular stomatitis virus glycoprotein: a transducing coat for SFV-based RNA vectors. J. Gene Med. 6 (9), 1014–1022.

Durham, A., 1972. Structures and roles of the polymorphic forms of the tobacco mosaic virus protein: I. Sedimentation studies. J. Mol. Biol. 67, 289–305.

Durham, A.C.H., Klug, A., 1971. Polymerization of tobacco mosaic virus protein and its control. Nat. New Biol. 229, 42–46.

Fleeton, M.N., Liljestrom, P., Sheahan, B.J., Atkins, G.J., 2000. Recombinant Semliki Forest virus particles expressing louping ill virus antigens induce a better protective response than plasmid-based DNA vaccines or an inactivated whole particle vaccine. J. Gen. Virol. 81, 749–758.

Fraenkel-Conrat, H., 1957. Degradation of tobacco mosaic virus with acetic acid. Virology 4, 1–4.

Fraenkel-Conrat, H., Singer, B., 1959. Reconstitution of tobacco mosaic virus III. Improved methods and the use of mixed nucleic acids. Biochim. Biophys. Acta 33, 359–370.

Hoare, M., Levy, M.S., Bracewell, D.G., Doig, S.D., Kong, S., Titchener-Hooker, N., Ward, J.M., Dunnill, P., 2005. Bioprocess engineering issues that would be faced in producing a DNA vaccine at up to 100 m (3) fermentation scale for an influenza pandemic. Biotechnol. Progr. 21 (6), 1577–1592.

Levy, M.S., O'Kennedy, R.D., Ayazi-Shamlou, P., Dunnill, P., 2000. Biochemical engineering approaches to the challenges of producing pure plasmid DNA. Trends Biotechnol. 18 (7), 296–305.

Loor, F., 1967. Comparative immunogenicities of tobacco mosaic virus, protein subunits, and reaggregated protein subunits. Virology 33, 215–220.

Lundstrom, K., 2002. Alphavirus-based vaccines. Curr. Opin. Mol. Ther. 4 (1), 28–34.

Lundstrom, K., 2005. Biology and application of alphaviruses in gene therapy. Gene Ther. 12, S92–S97.

Magnusson, M., Hong, S., Boulanger, P., Lindholm, L., 2001. Genetic retargeting of adenovirus: novel strategy employing "deknobbing" of the fiber. J. Virol. 75 (16), 7280–7289.

Martin, T., Parker, S.E., Hedstrom, R., Le, T., Hoffman, S.L., Norman, J., Hobart, P., Lew, D., 1999. Plasmid DNA malaria vaccine: the potential for genomic integration after intramuscular injection. Hum. Gene Ther. 10 (5), 759–768.

McCormick, A., Corbo, T., Wykoff-Clary, S., Nguyen, L., Smith, M., Palmer, K., Pogue, G., 2006. TMV-peptide fusion vaccines induce cell mediated immune responses and tumor protection in two models. Vaccine 24 (40–41), 6414–6423.

Morris-Downes, M.M., Phenix, K.V., Smyth, J., Sheahan, B.J., Lileqvist, S., Mooney, D.A., Liljestrom, P., Todd, D., Atkins, G.J., 2001. Semliki Forest virus-based vaccines: persistence, distribution and pathological analysis in two animal systems. Vaccine 19 (15–16), 1978–1988.

Nishikawa, M., Huang, L., 2001. Nonviral vectors in the new millennium: delivery barriers in gene transfer. Hum. Gene Ther. 12 (8), 861–870.

Oukka, M., Cohen-Tannoudji, M., Tanaka, Y., Babinet, C., Kosmatopoulos, K., 1996. Medullary thymic epithelial cells induce tolerance to intracellular proteins. J. Immunol. 156 (3), 968–975.

Piedra, P.A., 2003. Clinical experience with respiratory syncytial virus vaccines. Pediatr. Infect. Dis. J. 22 (2), S94–S99.

Pogue, G.P., Lindbo, J.A., Garger, S.J., Fitzmaurice, W.P., 2002. Making an ally from an enemy: plant virology and the new agriculture. Annu. Rev. Phytopathol. 40, 45–74.

Rotzschke, O., Falk, K., Stevanovic, S., Jung, G., Walden, P., Rammensee, H.G., 1991. Exact prediction of a natural T-cell epitope. Eur. J. Immunol. 21 (11), 2891–2894.

Sambrook, J., Fritsch, E., Maniatis, T., 1989. Molecular Cloning: A. Laboratory Manual. CSH Laboratory, New York.

Sin, J.I., Bagarazzi, M., Pachuk, C., Weiner, D.B., 1999. DNA priming-protein boosting enhances both antigen-specific antibody and Th1-type cellular immune responses in a murine herpes simplex virus-2 gD vaccine model. DNA Cell Biol. 18 (10), 771–779.

Smerdou, C., Liljestrom, P., 1999. Two-helper RNA system for production of recombinant Semliki Forest virus particles. J. Virol. 73 (2), 1092–1098.

Smith, M., Lindbo, J., Dillard-Telm, S., Brosio, P., Lasnik, A., McCormick, A., Nguyen, L., Palmer, K., 2006. Modified Tobacco mosaic virus particles as scaffolds for display of protein antigens for vaccine applications. Virology 348, 475–488.

Soleimanjahi, H., Roostaee, M.H., Rasaee, M.J., Mahboudi, F., Kazemnejad, A., Bamdad, T., Zandi, K., 2006. The effect of DNA priming-protein boosting on enhancing humoral immunity and protecting mice against lethal HSV infections. FEMS Immunol. Med. Microbiol. 46 (1), 100–106.

Stussi, C., Lebeurier, G., Hirth, L., 1969. Partial reconstitution of tobacco mosaic virus. Virology 38, 16–25.

Turner, D., Joyce, L., Butler, P., 1988. The tobacco mosaic virus assembly origin RNA. Functional characteristics defined by directed mutagenesis. J. Mol. Biol. 203 (3), 531–547.

Vilalta, A., Mahajan, R.K., Hartikka, J., Rusalov, D., Martin, T., Bozoukova, V., Leamy, V., Hall, K., Lalor, P., Rolland, A., Kaslow, D.C., 2005. I. Poloxamer-formulated plasmid DNA-based human cytomegalovirus vaccine: evaluation of plasmid DNA biodistribution/persistence and integration. Hum. Gene Ther. 16 (10), 1143–1150.

Wang, Z., Troilo, P.J., Wang, X., Griffiths, T.G., Pacchione, S.J., Barnum, A.B., Harper, L.B., Pauley, C.J., Niu, Z., Denisova, L., Follmer, T.T., Rizzuto, G., Ciliberto, G., Fattori, E., Monica, N.L., Manam, S., Ledwith, B.J., 2004. Detection of integration of plasmid DNA into host genomic DNA following intramuscular injection and electroporation. Gene Ther. 11 (8), 711–721.

Ying, H., Zaks, T.Z., Wang, R.F., Irvine, K.R., Kammula, U.S., Marincola, F.M., Leitner, W.W., Restifo, N.P., 1999. Cancer therapy using a self-replicating RNA vaccine. Nat. Med. 5 (7), 823–827.

Zhou, X., Berglund, P., Rhodes, G., Parker, S.E., Jondal, M., Liljestrom, P., 1994. Self-replicating Semliki Forest virus–RNA as recombinant vaccine. Vaccine 12 (16), 1510–1514.

Zhou, X.Z., Berglund, P., Zhao, H.X., Liljestrom, P., Jondal, M., 1995. Generation of cytotoxic and humoral immune-responses by nonreplicative recombinant Semliki-Forest-virus. Proc. Natl. Acad. Sci. U.S.A. 92 (7), 3009–3013.